

Convective Heat Transfer and Reference Free-stream Temperature Determination near the Casing of an Axial Flow Turbine

B. Gumusel² and C. Camci¹

Turbomachinery Aero-Heat Transfer Laboratory
Department of Aerospace Engineering
The Pennsylvania State University
223 Hammond Building, University Park, PA 16802

ABSTRACT

The present study explains a steady-state method of measuring convective heat transfer coefficient on the casing of an axial flow turbine. The goal is to develop an accurate steady-state heat transfer method for the comparison of various casing surface and tip designs used for turbine performance improvements. The free-stream reference temperature, especially in the tip gap region of the casing varies monotonically from the rotor inlet to rotor exit due to work extraction in the stage. In a heat transfer problem of this nature, the definition of the free-stream temperature is not as straight forward as constant free-stream temperature type problems. The accurate determination of the convective heat transfer coefficient depends on the magnitude of the local free-stream reference temperature varying in axial direction, from the rotor inlet to exit. The current study explains a strategy for the simultaneous determination of the steady-state heat transfer coefficient and free-stream reference temperature on the smooth casing of a single stage rotating turbine facility. The heat transfer approach is also applicable to casing surfaces that have surface treatments for tip leakage control. The overall uncertainty of the method developed is between 5 % and 8 % of the convective heat transfer coefficient.

¹ Cengiz Camci, Prof. of Aerospace Engineering, ASME fellow
² Baris Gumusel, Graduate Research Assistant

INTRODUCTION

Convective heat transfer to the static casing of a shroudless HP turbine rotor is a complex aero-thermal problem. The unsteady flow with a relatively high Reynolds number in the tip gap region has strong dependency on the tip clearance gap, blade tip profile; tip loading conditions, tip geometry and casing surface character. Thermal transport by flow near the casing inner surface is influenced by the unsteadiness, the surface roughness character and the turbulent flow characteristics of the fluid entering into the region between the tip and casing. Since the turbine inlet temperatures are continuously elevated to higher levels, casing and tip related heat transfer issues are becoming more critical in design studies.

In gas turbines, the gas stream leaving the combustor is not at a uniform temperature in radial and circumferential directions. According to Butler et al [1] the combustor exit maximum temperature can be twice as high as the minimum temperature. The maximum temperature in general is around the mid-span and the lowest gas temperatures are near the walls. The mechanisms related to the distortion of the radial temperature profile as the combustor exit fluid passes through a turbine rotor are complex, as explained by Sharma and Stetson [2] and Harvey [3]. The hottest part of the fluid leaving the upstream nozzle guide vane tends to migrate to the rotor tip corner near the mid pressure surface of the blade. Unfortunately, mostly the hottest fluid originating from the mid span region of the combustor or NGV finds its way to the pressure side corner of the blade tip in the rotating frame. Details of hot streak migration in gas turbines can be found in Roback&Dring [4,5], Takanashi&Ni [6], Dorney et al. [7] and Dorney&Schwab [8].

Due to significant energy extraction in a HP turbine stage, rotor absolute total temperature monotonically decreases in axial direction at a significant rate. This is especially true at the core of the blade passage where most of the energy extraction takes place. However, the fluid finding its way to the area between the casing and blade tips do not participate in the work generation as much as the mid-span fluid. Therefore, it is reasonable to accept that the near-casing fluid does not cool as much as the mid-span fluid when it progresses from rotor inlet to exit.

Yoshino [9] and Thorpe et al. [10] have shown that a rotor blade can also perform work on the fluid near the casing surface by means of “rotor compressive heating”. They obtained time-accurate and phase-locked casing heat flux measurements in Oxford Rotor Facility to show the casing heat loads as the rotor blades move relative to the static casing. They observed a very high heat flux zone on the casing inner surface for each blade in the rotor. Phase-locked measurements clearly indicated that the hot spot moved along the casing with the rotor. The results of this study showed two distinct levels of casing heating, one level for the casing interaction with the tip leakage fluid and a relatively low level for the casing interaction with the passage fluid located between blade tips. Thorpe et al. [10] explained the high heat flux zone on the casing surface by a “rotor compressive heating” model. They showed that the static pressure field near the tip can do work on the leakage fluid trapped between the blade tip and the casing. The “rotor compressive heating” model predicts that the absolute total temperature of the leakage fluid may exceed that of the rotor inlet flow. The flow near the casing turns and accelerates the leakage fluid to a tangential velocity level that is measurably above the rotor inlet level. Thorpe et al. [11] were successful in predicting the total temperature penalty due to compressive heating using the Euler work equation. Any design effort that will reduce the tip leakage mass flow rate in an axial turbine will also result in the reduction of the total temperature penalty and a corresponding reduction in casing heat load.

Past studies show three significant contributors to casing heat loads in shroudless HP turbines.

1. Radially outward and axial migration of a hot streak in each passage results in the accumulation of relatively high temperature fluid near the pressure side corner of the blade tip before it enters the tip gap.
2. A relatively higher total temperature in the near-casing fluid is observed because the near casing fluid does not participate in stage work generation. The leakage fluid does not expand as much as the core-flow in the rotor passage.
3. Rotor compressive heating performed by blade tips when they move against the static casing is significant.

The near-casing gas temperature drops at a significant rate in axial direction. There is also a strong circumferential mixing near the casing because of the relative motion of blade tips. The time accurate wall heat flux measured on the casing vary between a “passage gas induced low value” and “tip leakage fluid induced high value”. Since near-casing gas temperatures vary at a significant rate in axial direction, any heat transfer measurement approach requires the simultaneous measurement of this local gas temperature in the vicinity of the casing, in addition to an accurate determination of convective heat transfer coefficient.

A steady state casing heat/mass transfer coefficient measurement method based on a Naphthalene sublimation technique is explained in Rhee and Cho [12]. They report similar casing heat transfer distributions with and without blade rotation. Their sublimation based heat transfer method is inherently intrusive because of the variations of the Naphthalene layer thickness imposed by local mass transfer rate variations in the tip gap region.

The present paper explains a steady-state method for the simultaneous determination of the casing heat transfer coefficient and the free-stream reference temperature using a smooth casing in a single stage rotating turbine facility. The heat transfer approach is also applicable to casing surfaces with special surface treatments implemented for tip vortex de-sensitization. An uncertainty analysis follows a detailed description of the casing heat transfer measurements performed on a smooth casing surface.

EXPERIMENTAL SETUP & OPERATION

Turbine Research Facility: The facility used for the current casing heat transfer study, shown in Figure 1 is the Axial Flow Turbine Research Facility (AFTRF), at the Pennsylvania State University. A detailed description of the operational characteristics of this rotating rig is available in Camci [11]. The research facility is a large-scale, low speed, cold flow turbine stage depicting many characteristics of modern high-pressure turbine stages. The total pressure and total temperature ratios across the stage are presented in Table 1 and air flow through the facility is generated by a four stage axial

fan located downstream of the turbine. The rotor hub extends 1.7 blade tip axial chord length beyond the rotor exit plane. The turbine rig has a precision machined removable casing segment for measurement convenience especially for casing related aero-thermal studies.

Table 1 AFTRF Facility Design Performance Data

Inlet Total Temperature: T_{o1} (K)	289
Inlet Total Pressure: P_{o1} (kPa)	101.36
Mass Flow Rate: Q (kg/sec)	11.05
Rotational Speed: N (rpm)	1300
Total Pressure Ratio: P_{o1}/P_{o3}	1.077
Total Temperature Ratio: T_{o3}/T_{o1}	0.981
Pressure Drop: $P_{o1}-P_{o3}$ (mm Hg)	56.04
Power: P (kW)	60.6

A few of the relevant design performance data are listed in Table 1, while Table 2 lists important blade design parameters, including reaction at blade hub and tip sections, Reynolds number at rotor exit and a few blade parameters. Measured/design values of rotor inlet flow conditions including radial, axial, tangential components and data acquisition details of the turbine rig are explained in detail by Camci [13] and Rao et al. [14].

Instrumentation: Instruments used for monitoring the performance parameters of AFTRF consist of total pressure probes, Kiel probes, pitot-static probes, thermocouples, and a precision in-line torquemeter. The turbine rotational speed is kept constant around 1300 rpm by means of an eddy current brake.

Removable Turbine Casing: Figure 1.b shows the facility removable casing segment as a convenient feature of the test facility. A rectangular window is used to house the removable casing segment. This segment is a precision machined area designed for many different areothermal measurement techniques to be applied around the turbine stage. Tip clearance is measured via a set of precision shim gages between the AFTRF casing and

individual blade tip surfaces. The position of the aluminum plate with respect to the AFTRF casing is also accurately determined.

Table 2 AFTRF Stage Blade & Vane Data

Rotor hub-tip ratio	0.7269
Blade Tip Radius; R_{tip} (m)	0.4582
Blade Height; h (m)	0.1229
Relative Mach Number	0.24
Number of Blades	29
Axial Tip Chord; (m)	0.085
Spacing; (m)	0.1028
Turning Angle; Tip / Hub	95.42° / 125.69°
Nominal Tip Clearance; (mm)	0.9
Reaction, Hub / Tip	0.197 / 0.519
Reynolds Number ($\div 10^5$) inlet / exit	(2.5~4.5) / (5~7)

Figure 2 shows the removable segment with the rectangular central area (dashed boundaries Figure 1.b) allowing the researchers to perform casing heat transfer measurements. The “smooth” aluminum casing plate that is facing the rotor tip and interacting with near-casing fluid is also shown in Figures 2 and 3. The Al casing plate could easily be replaced with custom made plates having special casing treatments for tip vortex aerodynamic de-sensitization and supporting heat transfer studies. The removable turbine casing and the Al plate are carefully designed and precision machined so that many subsequent installations of the same Al plate and the removable window/casing result in a repeatable tip clearance. Tip clearance repeatability within $\pm 25 \mu\text{m}$ (± 0.001 inch) for a blade height of 125 mm (4.85 inches) is possible. This uncertainty corresponds to a change in non-dimensional tip clearance of $\pm 0.02\%$ of the blade height. Under normal circumstances, the inserted Al plate is supposed to be flush with the static casing of the facility. Slight clearance adjustments are possible for the removable segment by altering the thickness of the “plastic insulator” as shown in Figure 3. The baseline Al casing plate has consistent radius of curvature with the casing. The average turbine tip clearance for the current experiments is kept at $t/h=0.76\%$.

Heat Transfer Coefficient Measurement Locations: The five convective heat transfer coefficient measurement locations are shown in Figure 4. Location 1 is closest to the leading edge of the blade in axial direction. The five selected measurement locations cover the axial distance between the blade leading edge and slightly downstream of the trailing edge. Due to the rotation of the blade, the steady-state heat transfer coefficient distribution in circumferential direction is reasonably uniform. Since work is extracted in the rotor, the free-stream total temperature between the rotor inlet and rotor exit are different. Free-stream total temperature measurement locations at the turbine inlet, rotor inlet, rotor exit and turbine exit are also shown in Figure 4. The free-stream total temperatures at turbine inlet and exit are measured using calibrated K type thermocouples in a Kiel probe arrangement. Rotor inlet and exit thermocouples are inserted into the flow at about 25 mm away from the casing surface.

Steady-state Heat Transfer Method: Casing convective heat transfer coefficients and corresponding free-stream reference temperatures are measured simultaneously with the help of a constant heat flux heater as shown in Figure 5. A constant heat flux heater (*MINCO Corp. HK5175R176L12B*) with an effective area of ($A=76 \times 127 \text{ mm}^2$) is sandwiched between two thin Mylar sheets. The heater can produce a maximum of 75 Watts with an overall resistance of 176 ohms. The overall resistance of the 0.5 mm thick heater has extremely small temperature dependency in the range of the current experiments. This resistance value is continuously measured and recorded during each measurement. The Joule heating value in the heater is I^2R/A [Watts/m²]. The heat transfer surface has many flat ribbon thermocouples of type K imbedded at many locations (symbol □ in Figure 5).

Table 3 Thermal conductivity and thickness values for the heat transfer surface components

MATERIAL	Thermal Conductivity W/m-K	Thickness mm [inch]
ROHACELL	0.030	4.064 [0.160]
ALUMINUM PLATE	202.4	0.762 [0.030]
PLASTIC LAYER	0.120	1.397 [0.055]
HEATER (Minco)	0.981	0.500 [0.021]

The flat thermocouple junctions are 12 μm thick. There are two thick layers of Rohacell insulating material flush mounted on top of the heater surface. Table 3 includes the material thicknesses in the heat transfer composite surface and thermal conductivity values. Current multi-dimensional heat conduction analysis shows that the lateral conduction of thermal energy at the edges of the heater surface and Rohacell insulator are extremely small and negligible. However the heat conduction loss q_{loss} in Rohacell is not negligible in a direction normal to the heater,

$$q_{loss} = (T_H - T_{RH})/(L_{RH}/k_{RH}) \quad (1)$$

Due to extremely thin structure and the uniform internal heat generation by Joule heating in the volume of the heater, measured top and bottom surface temperatures T_H are very close to each other. The amount of heat flux conducted through the aluminum casing plate in a direction normal to the plate is

$$q_{conv} = I^2 R/A - q_{loss} = (T_H - T_f)/(L_{Al}/k_{Al} + 1/h) = (T_w - T_f)/(1/h) \quad (2)$$

Equation (2) shows convective heat flux crossing the fluid-solid interface on the casing surface when the lateral conduction losses in Al plate are ignored. Equation (2) also presents the convective heat transfer rate written between the heater T_H and the near-casing turbine fluid T_f . In this approach, a heat transfer coefficient h can be measured without measuring the wall temperature T_w directly. h is first calculated from Equation (2) between T_H and T_f . The corresponding wall temperature T_w is then obtained from the last part of Equation (2) written between the wall and free stream,

$$T_w = T_H - q_{conv} \cdot (L_{Al}/k_{Al}) \quad (3)$$

The specific experimental approach in finding T_w is useful since a non-intrusive wall temperature measurement at the fluid-casing interface is essential for this problem. A more accurate form of h can be obtained by quantifying lateral conduction losses in the aluminum plate. A three dimensional conduction heat transfer analysis including all

complex geometrical features of the removable turbine casing is presented in the next few paragraphs. This computational effort reduces the measurement uncertainties in the measured convective heat transfer coefficient h . The correction is based on calculating the lateral conduction losses in the casing plate.

Lateral Conduction Losses in Aluminum Casing Plate: Figure 6 presents the results from a 3D heat conduction analysis for the removable turbine casing. The removable turbine casing is an extremely thick precision machined aluminum with an average thickness of 50.8 mm (about 2 inches). The lateral heat conduction in the aluminum casing plate in this experiment was deduced from a 3D heat conduction analysis performed under realistic thermal boundary conditions. The steady-state thermal conduction equation $\nabla^2 T(x, y, z) = 0$ was solved in the removable turbine casing with proper boundary conditions.

The constant heat flux heater shown in Figure 5 is operated at a prescribed power I^2R [W] value. Joule heating in the heater was simulated by distributing this I^2R value uniformly over the volume of the thin heater as an internal heat generation term. This is achieved by adding a source term to the energy equation in the numerical solution procedure.

Boundary Conditions for Conduction Loss Analysis: On the turbine flow side, the surface temperature upstream of the rotor leading edge is taken as the measured turbine rotor inlet temperature (or NGV exit temperature). The flow side surface temperature downstream of the rotor trailing edge is the same as the measured rotor exit temperature. The flush mounted aluminum casing plate has a convective type boundary condition on the flow side where a typical heat transfer coefficient h and a free-stream reference temperature is specified at five axial positions. Measured ambient temperature outside the rig is specified on the external flat face of the removable turbine casing. All other boundaries on the side walls were taken as adiabatic. The heater surface area is about the same area as that of the small rectangular cut shown in Figure 6.a.

Lateral Conduction Analysis Results: The temperature distribution on the Al casing plate as shown in Figure 6 facing the rotating blade tips is characterized by the red zone on top of the heater area. Along the dashed line in the measurement area (in axial direction) the temperature distribution is reasonably uniform within 0.5 °K. The

minimum and maximum temperatures in Figures 6 and 7 are 310 °K (blue) and 317 °K (red). All red hues are approximately corresponding to an area of 1 ° K temperature band.

Figure 7.a shows the plastic spacer/insulator inserted between the removable turbine casing shown in Figure 6.a and the 0.030 inch thick aluminum plate. The heater is flush mounted on the convex side of the aluminum plate. Two layers of Rohacell insulator were located on top of the heater surface in order to reduce the heat losses to the ambient from the heater as shown in Figure 5. The low conductivity plastic spacer is essential in this measurement approach in reducing the heat losses in the 0.030 inch thick casing plate. Figure 8 presents the lateral conduction heat losses from the aluminum casing plate. $Q_{ABCD} = (Q_A + Q_B + Q_C + Q_D)$ is the sum of all thermal energy (in Watts) laterally conducted from the rectangular area where the heater is flush mounted to the casing plate. Q_{RH} is the heat loss through the Rohacell insulator and Q_{HS} is the heat loss from the extremely narrow side faces of the heater volume with a thickness of 0.5 mm.

A new heat loss calculation was performed for each power setting using the 3D conduction analysis with proper boundary conditions. Figure 8 shows that the heat losses through the Rohacell layer and from the sides of the thin heater are extremely small when compared to the lateral conduction in the aluminum plate and the convective heat flux to the near-casing fluid in the turbine passage. A proper correction of convection heat flux term q_{conv} in equation (2) using lateral conduction losses is an important part in obtaining heat transfer coefficient on the turbine casing surface. Figure 9 presents the variation of convective heat flow over area A [$q_{conv} \cdot A$], lateral conduction loss Q_{ABCD} in aluminum casing plate, Rohacell layer losses and heater side losses as a function of heater power setting I^2R . Rohacell layer heat losses and heater side losses are negligible when compared to the convective heat flux and lateral conduction loss.

Heat Transfer Coefficient from Different Power Settings: The convective heat transfer coefficient is measured by using an arranged form of equation (2),

$$h = \frac{q_{conv} k_{Al}}{k_{Al}(T_H - T_f) - L_{Al} q_{conv}} \quad (4)$$

where q_{conv} is obtained by subtracting the predicted heat loss q_{loss} from I^2R/A as shown in equation (2). T_H is measured from a flush mounted thermocouple imbedded between the heater and the Al casing plate as shown in Figure 5. A non-intrusive measurement of T_w is also available from Equation (3).

The Correct Free Stream Reference Temperature: Finding the most accurate value of the reference fluid temperature T_f in this problem is crucial. T_f is the reference free-stream fluid temperature in the immediate vicinity of the casing surface facing the blade tips. Since this temperature in a turbine rotor monotonically decreases from rotor inlet to exit, a linear curve fit is obtained from the measured rotor inlet $T_{R,inlet}$ and rotor exit $T_{R,exit}$ as shown in Figure 5. The two measurement thermocouples for $T_{R,inlet}$ and $T_{R,exit}$ are inserted into the free-stream before and after the rotor. The junctions are in the turbine flow at a location about 25 mm away from the casing surface. The open circular symbols shown in Figure 10 form an h measurement at axial location 1. A line fit passing from all circular symbols obtained from many different power settings is represented by $q_{conv}=h.(T_w-T_f)$ for the same turbine operating point. Maximum attention is paid to keep the corrected speed of the turbine facility and flow coefficient constant during the acquisition of all points at different heater power settings. The slope of this straight line is the convective heat transfer coefficient h .

The T_f value measured in the turbine free stream flow at this stage is not a proper reference temperature for this convective heat transfer problem. Since the thermocouples providing T_f are inserted well into the free stream (25 mm away from the casing) the measured local T_f are considerably different from the temperature of the fluid in the immediate vicinity of the casing. This observation is consistent with the data shown with circular symbols in Figure 10. The solid line connecting the circular symbols does not pass through the origin as $q_{conv}=h.(T_w-T_f)$ suggests. This is a clear indication of the fact that the initially measured T_f (defined by $T_{R,inlet}$ and $T_{R,exit}$) is not proper for the casing heat transfer problem. What happens when the solid line does not pass through is directly related to the observation made in Figure 11. The computation of h at many different power settings at the same turbine flow condition does not yield to an invariant h . The open triangular symbols suggest that h varies strongly with increased heater power setting.

Direct Measurement of T_{aw} as the Correct Free Stream Reference Temperature:

Using multiple heater power settings allows a simultaneous measurement of h and T_{aw} . h and $T_{aw}=T_f$ as two unknowns of $q_{conv}=h.(T_w-T_f)$ could be obtained from two independent measurement points obtained at two different power settings. Having many more points than two and using a first order line fit only reduces the experimental uncertainties in this process. The true reference temperature in this problem (adiabatic wall temperature T_{aw}) is obtained by shifting the original solid line to the left until it passes through the origin. The amount of this horizontal shift is the correction to be applied to initially suggested T_f . The corrected value of T_f is actually the same as the actual adiabatic wall temperature T_{aw} .

A Validation of T_{aw} measurement: A useful check on the value of h obtained from the measured reference temperature T_{aw} is shown in Figure 11. When h is calculated by using measured T_{aw} at many different power settings a constant level of h is obtained as shown by solid circular symbols. This constant level of h within experimental uncertainty indicates that the measured T_{aw} is the proper reference temperature for this convective heat transfer problem.

The procedure described in this section has the ability to measure the heat transfer coefficient h and free-stream reference temperature $T_f=T_{aw}$ simultaneously in a non-intrusive way. A direct measurement of T_{aw} in the turbine in the tip gap region by an inserted probe is extremely difficult. Another complexity is that the reference temperature continually drops in the turbine due to the work extraction process gradually building up in the axial direction. Figure 11 is a good display of the fact that the measured heat transfer coefficient h (slope of the solid line in Figure 10) is independently defined from the power setting and thermal boundary conditions $\Delta T=T_w-T_f$.

Axial Distribution of h on the Casing Plate: Figure 12 presents heat transfer coefficient data at all five axial locations defined in Figure 4. At this stage, q_{conv} is not corrected for lateral conduction losses yet. The same measurement methodology described in the previous paragraphs is applied at all five locations. A typical heat transfer experiment in AFTRF has an approximate duration of 50 minutes with h data obtained from 8 to 10 discrete heater power levels. No data is taken in the first 20 minutes to allow reasonably steady thermal and free-stream conditions to develop in AFTRF.

Figure 13 shows the axial distribution of h at five axial locations on the casing plate facing the blade tips. The solid circles represent the data before a lateral conduction correction in the aluminum casing plate is applied. The magnitude of lateral conduction losses are carefully determined from a 3D heat conduction analysis described in Figures 6 to 9. A proper heat loss analysis was performed for each power setting level carefully. A significant change in the overall magnitude of the heat transfer coefficients is observed after taking into account all energy losses from the Al casing plate, especially the lateral conduction losses. The casing plate measurement locations see the subsequent passage of tip leakage related fluid and passage fluid at blade passing frequency. The circumferential mixing in this near casing area is inevitable. A proper lateral conduction calculation is essential to reduce the experimental uncertainties in this heat transfer measurement approach.

Experimental Uncertainty Estimates: The most significant goal of this study was to establish a steady-state casing heat transfer measurement system with reduced uncertainties. Since the number of parameters to be controlled in the rotating rig is much larger than a typical wind tunnel study, a detailed uncertainty analysis is essential to control and reduce the experimental errors. The specific uncertainty approach follows the concepts developed by Kline and McClintock [15]. Our uncertainty analysis is based on our uncertainty estimates on reference free-stream temperature, heater surface temperature, thermal conductivity, plate thickness and aluminum casing lateral conduction error.

Table 4 Uncertainty estimates

QUANTITY	MEASUREMENT ERROR
T_f	$\delta T_f = \pm 0.15^{\circ} K$
T_H	$\delta T_H = \pm 0.15^{\circ} K$
k_{Al}	$\delta k_{Al} = \pm 0.221 W/m-K$
L_{Al}	$\delta L_{Al} = \pm 0.001" (25 micron)$
q_{conv}	$\delta q_{conv}/q_{conv} = \pm 1\% - 6\%$
h	$\delta h/h = \pm 5\% - 8\%$

Table 4 lists the magnitudes of all estimated basic measurement uncertainties. Uncertainty analysis showed that very low heater power levels typically less than 1 Watt have a tendency to increase $\delta h/h$. The lateral conduction loss could vary from 1 % to 6 % even after numerically correcting for the lateral heat conduction. This uncertainty is introduced to account for edge heat flux variations around a mean q_{conv} that already takes lateral conduction into account in a uniform way in axial direction. The uncertainty of heat transfer coefficient is estimated to be in a range from 5 % to 8 %.

CONCLUSIONS

A steady-state method for the measurement of convective heat transfer coefficient on the casing surface of an axial flow turbine is presented.

The current study presents a simultaneous measurement approach for both the heat transfer coefficient and the reference temperature of the near-casing fluid.

The non-intrusive determination of the reference near-casing fluid temperature $T_f = T_{aw}$ from the current method is highly effective in reducing the heat transfer measurement uncertainty.

The method developed is very suitable for research turbine applications where the free stream fluid continuously cools from rotor inlet to rotor exit due to work extraction.

Special attention is paid to the static casing region facing the rotor blades. The current T_{aw} measurement approach is a highly effective and non-intrusive approach for the fluid layers in the immediate vicinity of the static casing.

A significant improvement of the uncertainty of h is possible by taking lateral conduction losses in the casing plate into account. The lateral conduction losses resulting from each power setting of the “constant heat flux heater” were numerically evaluated on a high resolution 3D conduction grid prepared for the removable casing model.

The present method is able to take the variation of many turbine run time parameters into account during a 50 minute run in which at least 8-10 heater power settings are used for the measurements.

A detailed uncertainty analysis is presented. The current heat transfer measurement method uncertainty is estimated to be between 5 % and 8 % of convective heat transfer coefficient h .

The heat transfer evaluation of many casing surface modifications and blade tip shape modifications are possible with the specific method presented in this paper.

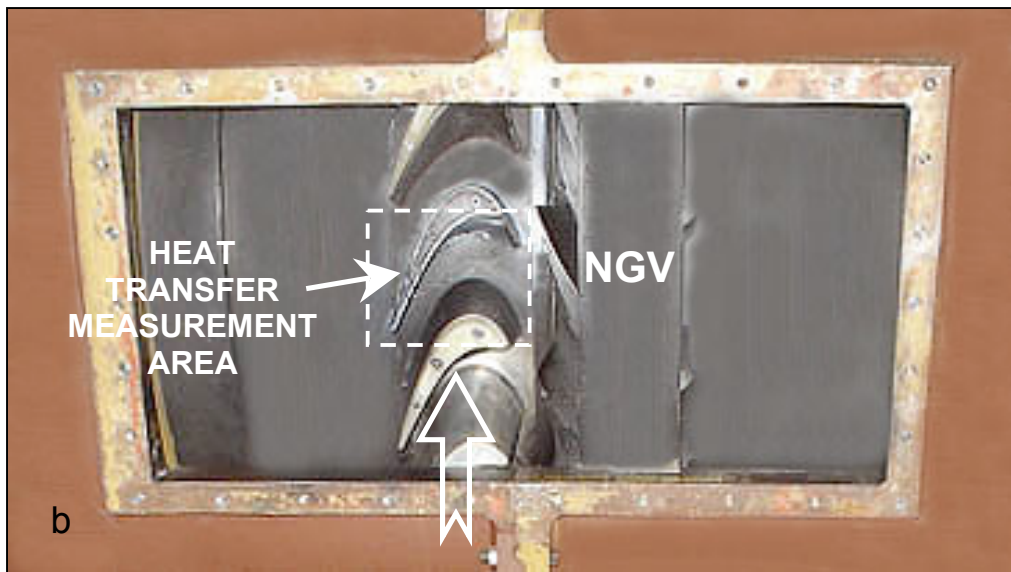
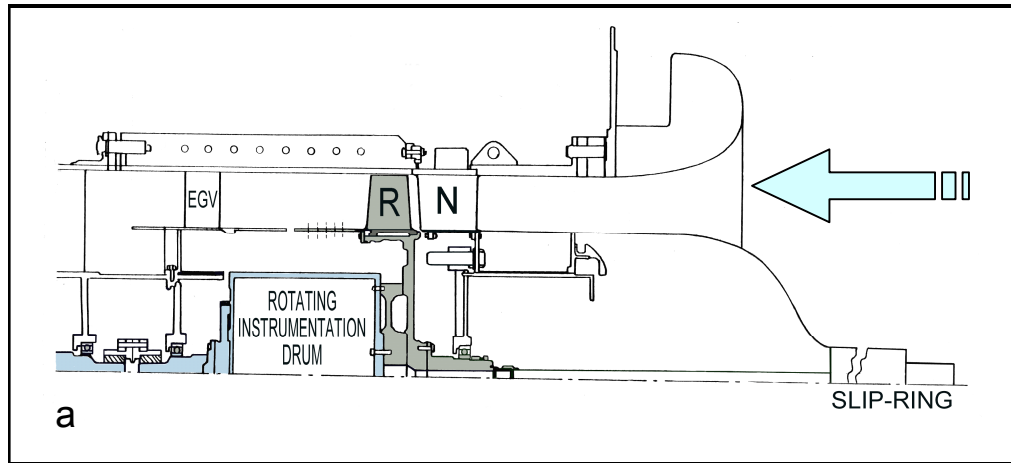


Figure 1 Axial Flow Turbine Research Facility (AFTRF)

a. facility schematic

b. window for the removable casing segment

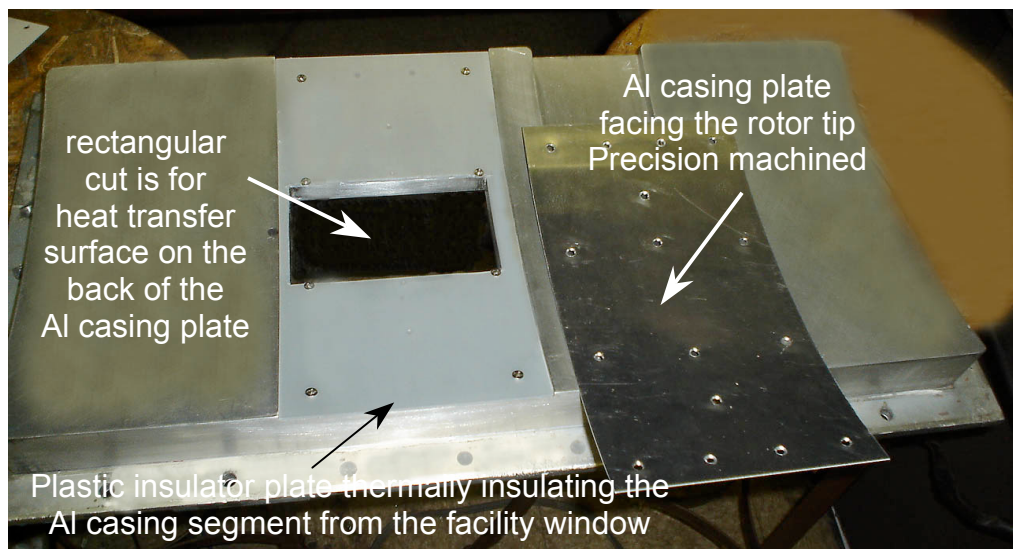
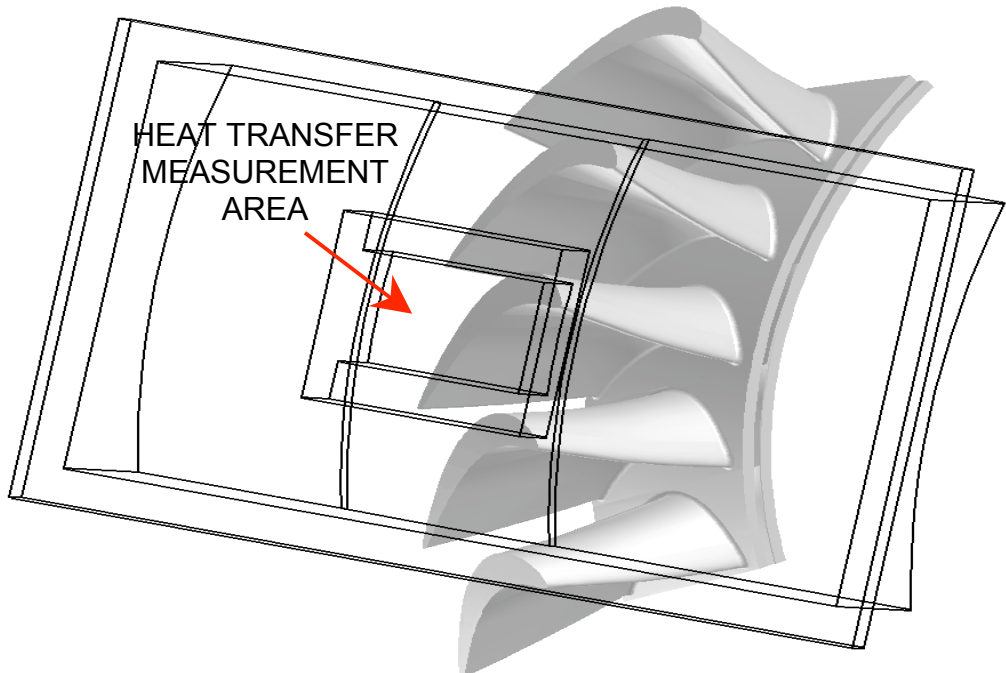


Figure 2 Removable turbine casing in (AFTRF)
(smooth partial “Al casing plate” is visible)

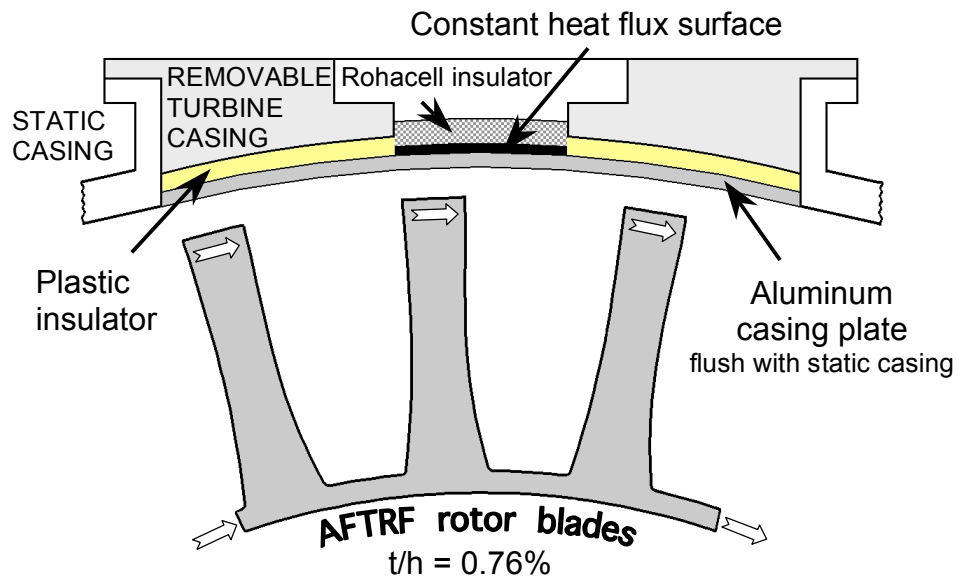


Figure 3 Removable turbine casing cross section
(normal to the axis of rotation)

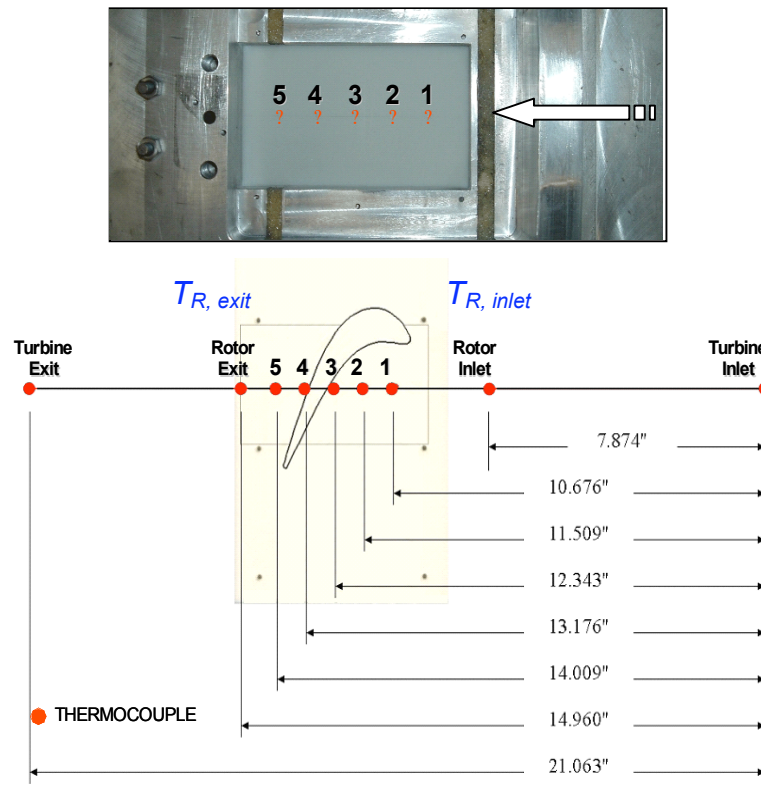


Figure 4 Heat transfer coefficient measurement locations on the casing surface
(five axial locations)

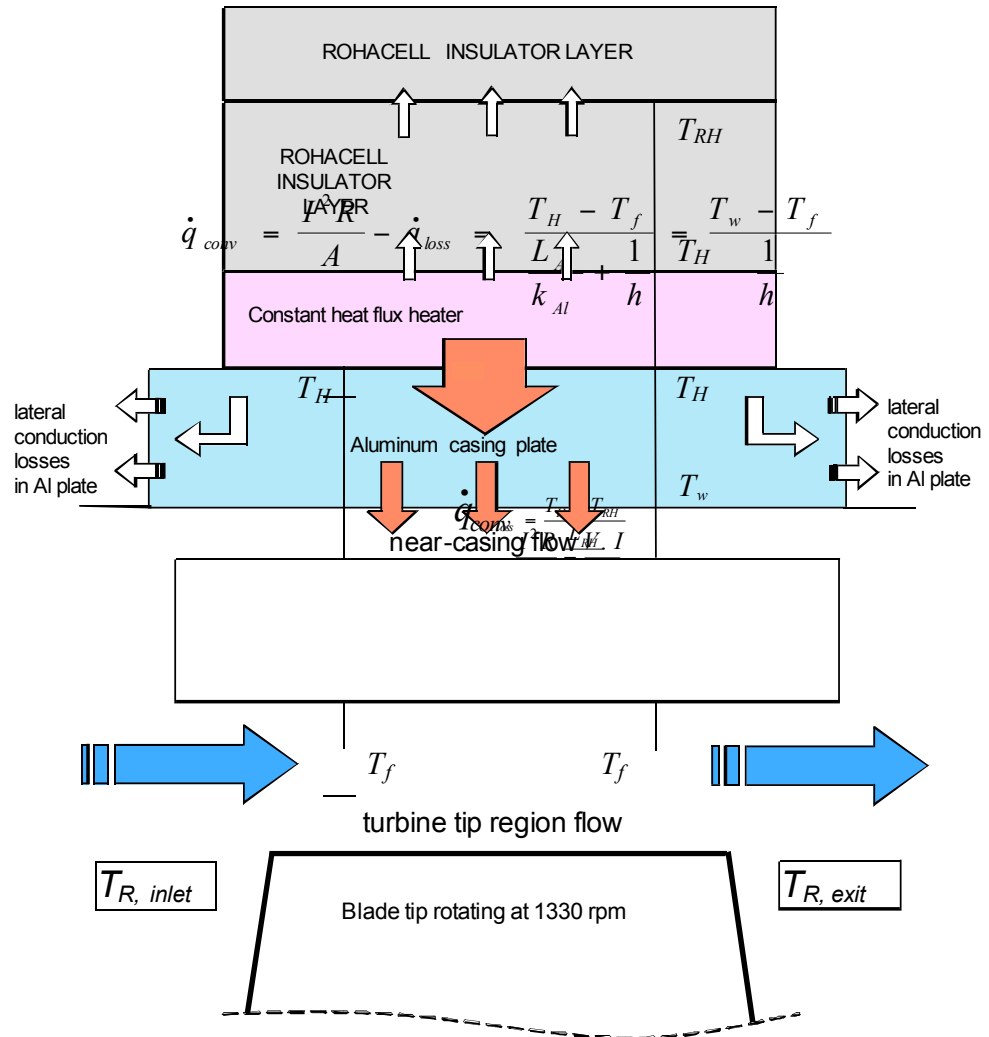


Figure 5 Heat Transfer model for convective heat transfer coefficient measurements on the turbine casing surface (the model allows for lateral conduction losses)

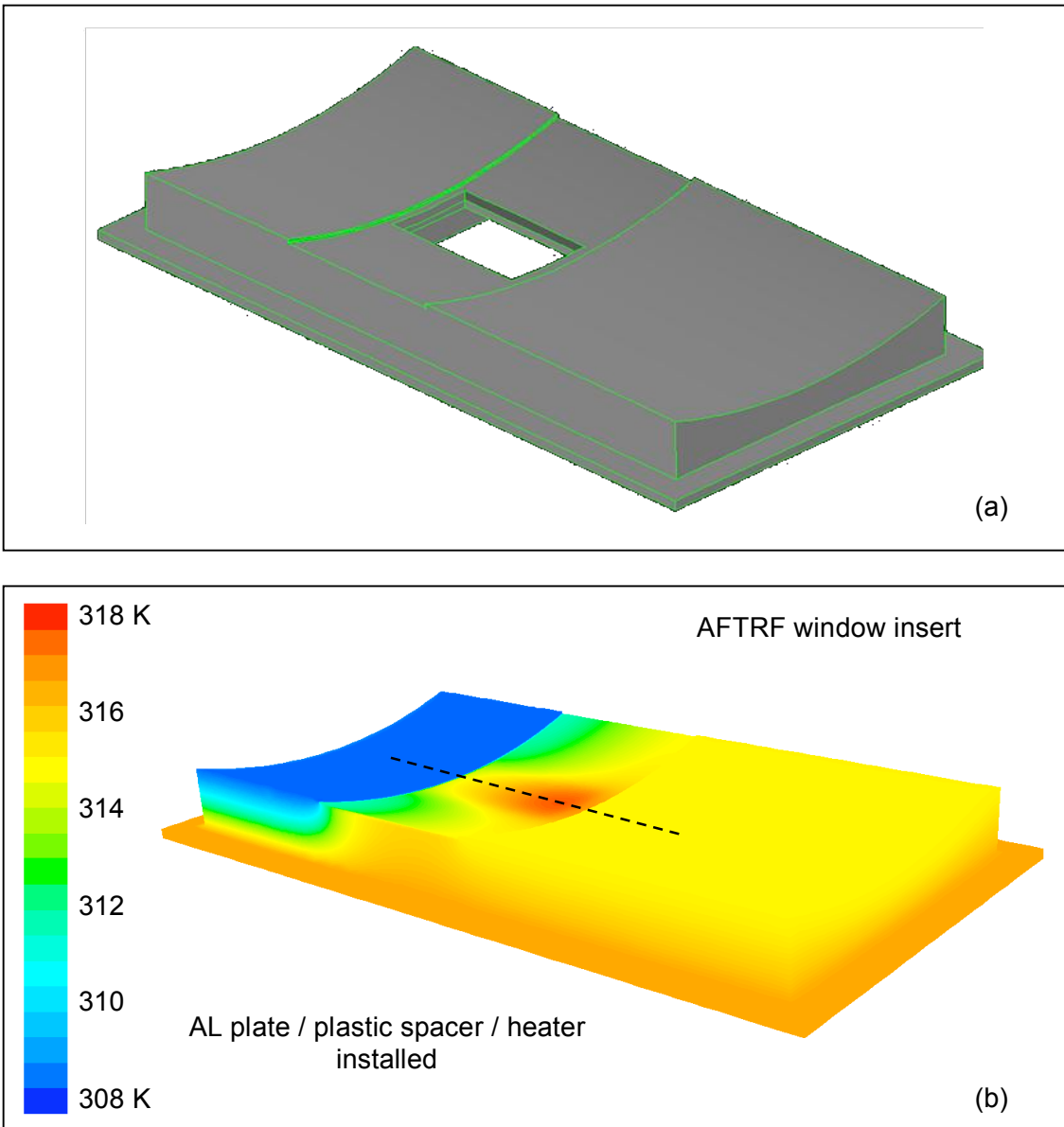
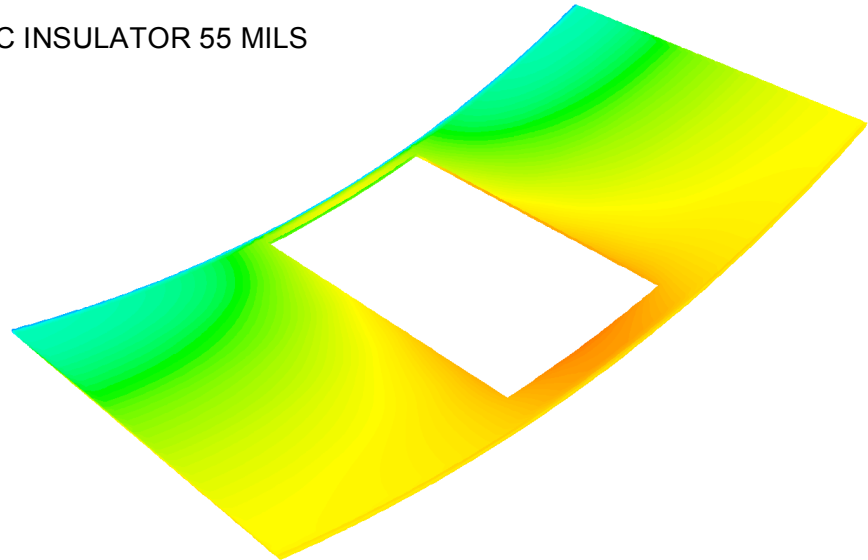


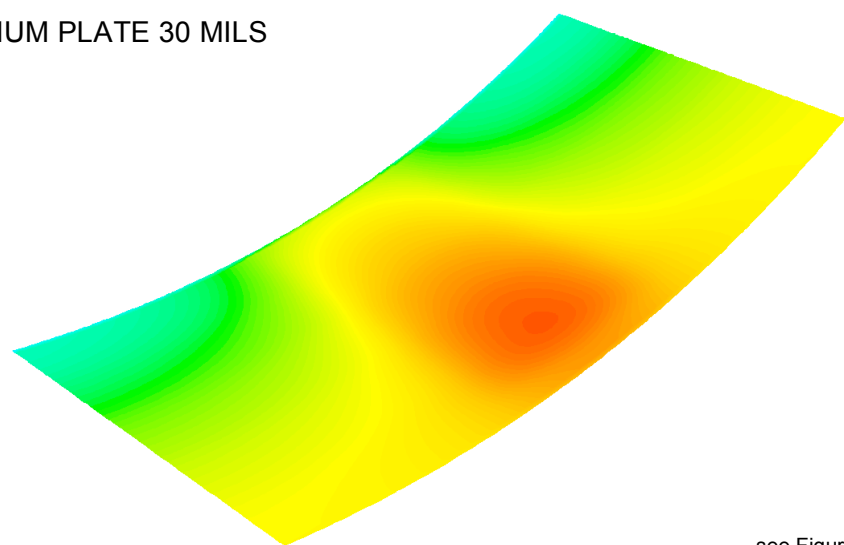
Figure 6 3D solid model and conduction analysis results on removable turbine casing surfaces

PLASTIC INSULATOR 55 MILS



(a)

ALUMINUM PLATE 30 MILS



(b)

see Figure 6 for legend

Figure 7 Temperature distributions on the plastic spacer and aluminum casing plate (flow side)

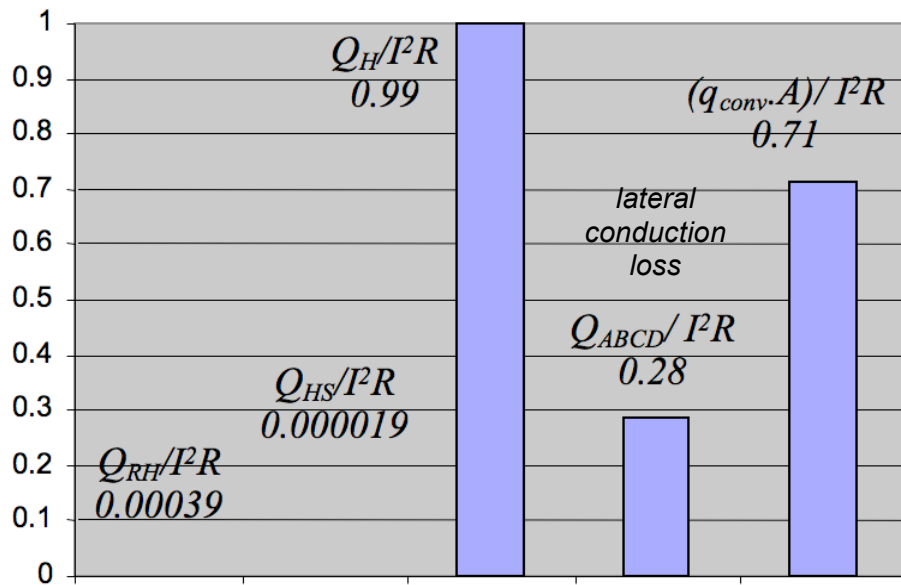
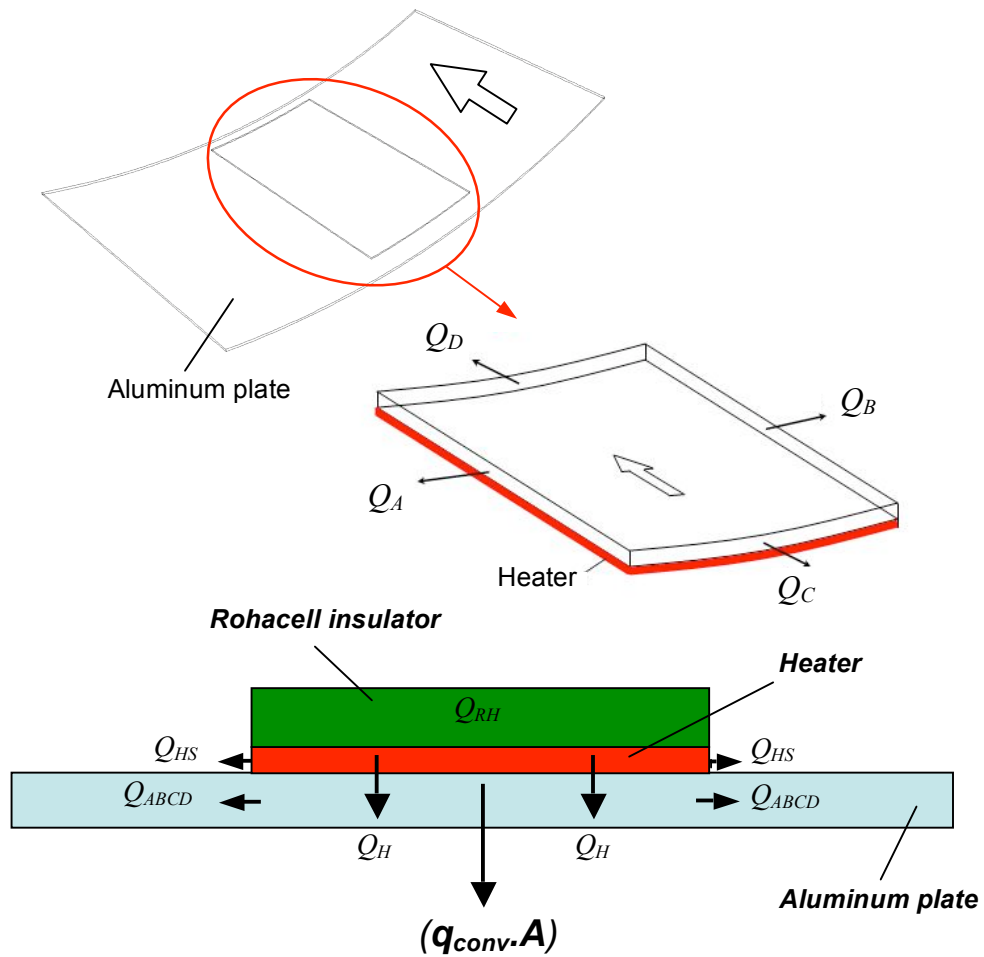


Figure 8 Lateral conduction from the four sides of the area facing the heater and the final energy balance ($\text{I}^2\text{R}=6.53 \text{ W}$)

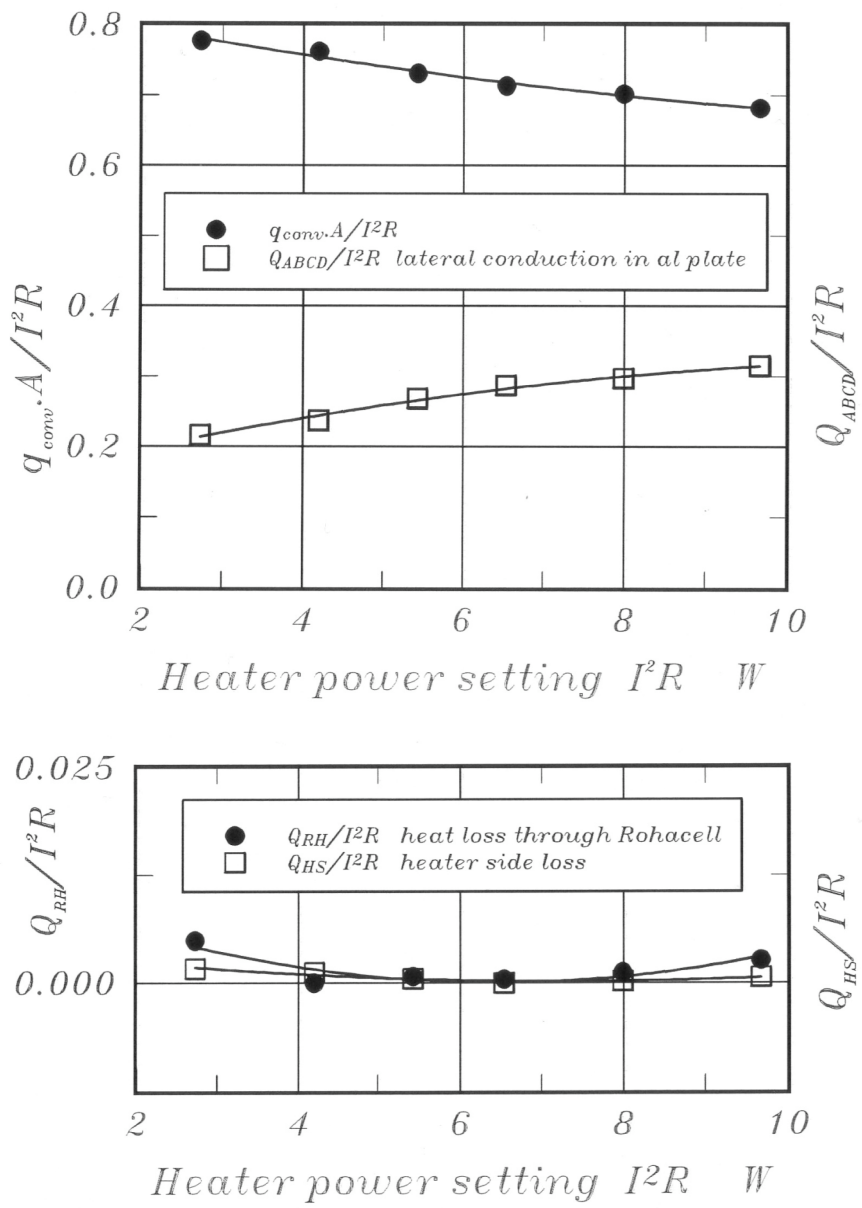


Figure 9 Energy balance in the heat transfer surface in function of power setting

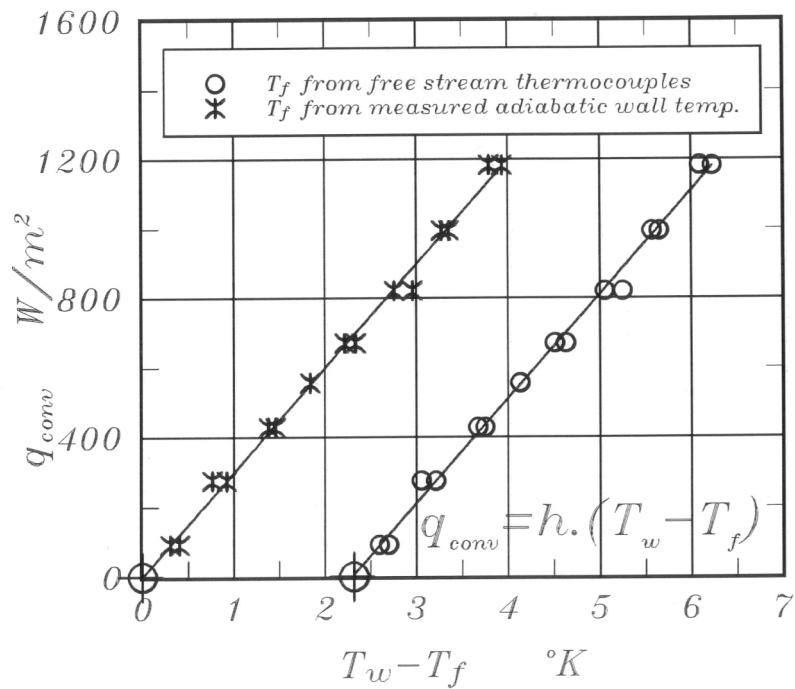


Figure 10 Simultaneous determination of convective heat transfer coefficient h and free stream reference temperature from multiple heater power settings

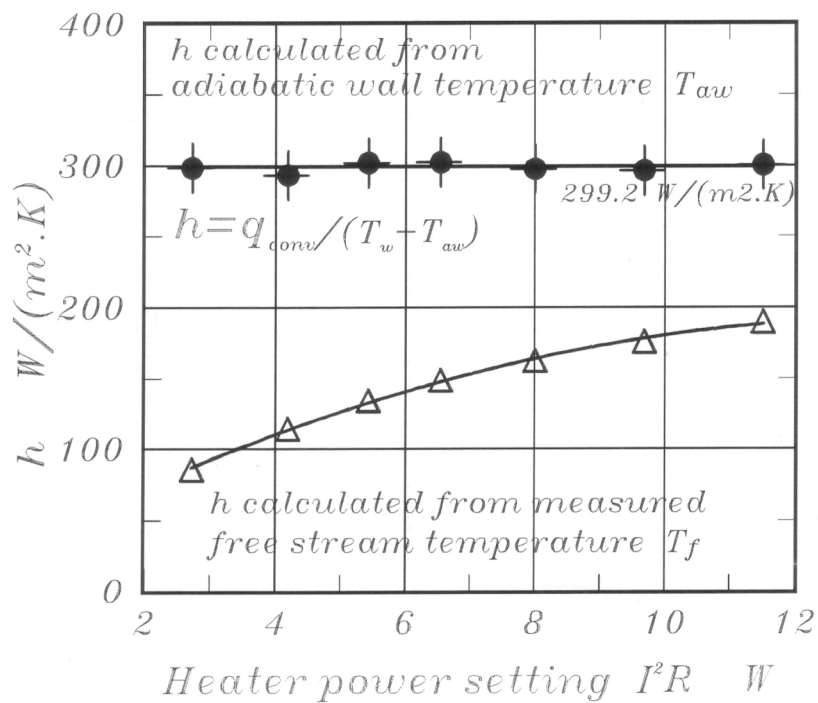


Figure 11 Influence of proper free stream reference temperature on convective heat transfer coefficient

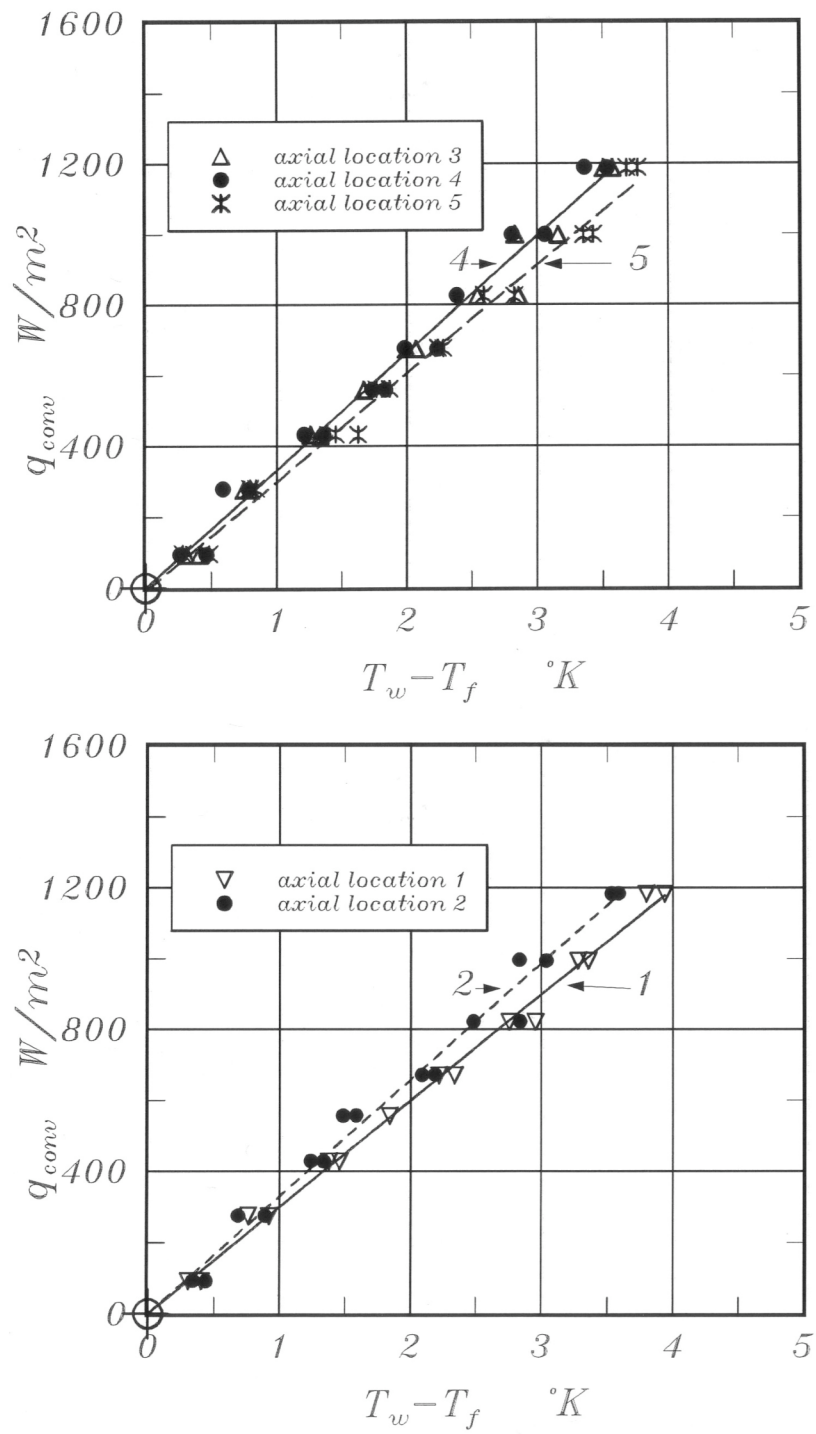


Figure 12 Measured heat transfer coefficient h (slope) at five axial locations on the casing plate surface

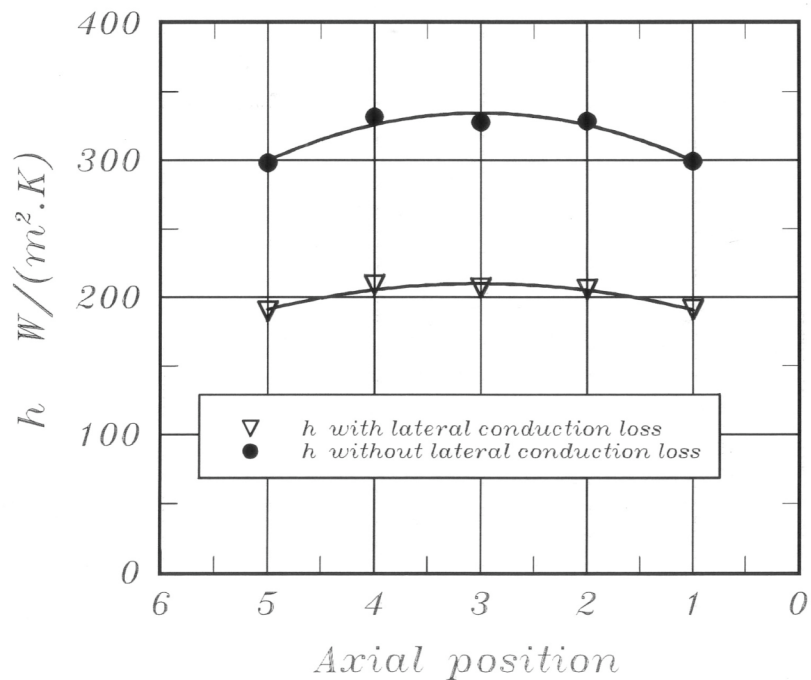


Figure 13 Distribution of the heat transfer coefficient with respect to axial position on the casing surface

ACKNOWLEDGMENTS

The authors acknowledge the valuable comments and advice provided by Dr. R.E.Chupp of GE Power Systems throughout this study. They are indebted to Mr.Harry Houtz, Rick Auhl, Mark Catalano, and Kirk Hellen for their technical support. The authors also acknowledge the valuable support from the Department of Aerospace Engineering at Penn State University.

NOMENCLATURE

A	heat transfer measurement area [m^2] also constant heat flux surface area
h	convective heat transfer coefficient [$\text{W}/\text{m}^2 \cdot \text{K}$]
h	also rotor blade height
I	DC current level to heater
I^2R	Joule heating in the heater [W]
k	thermal conductivity
L	material thickness
N	rotational speed [rpm]
P_{o1}	stage inlet total pressure, Pa
P_{o3}	stage exit total pressure, Pa
P	turbine power output [kW]
Q_{RH}	total heat flow through Rohacell insulator [W]
Q_{HS}	heat loss from the sides of the 0.5 mm thin heater [W]
$Q_H = (I^2R - Q_{RH} - Q_{HS})$	[W]
Q_{ABCD}	lateral conduction loss in al casing plate [W] (all four sides, see Figure 8)
q_{conv}	convective wall heat flux [W/m^2]
q_{loss}	heat loss to ambient (through Rohacell) [W/m^2]
$q_{conv.A}$	convective heat flow through area A $q_{conv.A} = (Q_H - Q_{ABCD})$ [W]
Q	turbine mass flow rate [kg/s]
r, R	radius
t	gap height between blade tip and outer casing
t/h	non-dimensional average tip clearance $t/h=0.76\%$
T_{o1}	stage inlet total temperature [K]
T_{o3}	stage exit total temperature [K]
T_{aw}	adiabatic wall temperature
T_f	Free stream reference temperature [T_{aw}]
$T_{R,inlet}$	free stream total temperature at rotor inlet (measured 1 25 cm away from casing)
$T_{R,exit}$	free stream total temperature at rotor exit (measured 1 25 cm away from casing)
U_m	rotor blade speed at mid-height location
V	velocity
V	also DC voltage applied to the heater
θ, x, r	tangential, axial, radial directions

subscripts

<i>aw</i>	adiabatic wall
<i>Al</i>	Aluminum
<i>f</i>	free stream fluid reference
<i>H</i>	heater
<i>RH</i>	Rohacell insulator material
<i>w</i>	wall

REFERENCES

1. Butler, T.L., Sharma O.P., Joslyn, H.T., Dring, R.P., 1989, "Redistribution of an inlet Temperature Distribution in an Axial Flow Turbine Stage", AIAA Journal of Propulsion, .Vol.5, No.1, pp.64-71.
2. Sharma, O.P., Stetson, G.M., 1998, "Impact of Combustor Generated Temperature Distortions on Performance, Durability and Structural Integrity of Turbines", VKI Lecture Series 1998-02, Feb.9-12, Brussels, Belgium.
3. Harvey, N.W., 2004, "Turbine Blade Tip Design and Tip Clearance Treatment", von Karman Institute Lecture Series VKI-LS 2004-02 ISBN 2-930389-51-6, Brussels.
4. Roback, R.J., Dring, R.P., 1992, "Hot Streaks and Phantom Cooling in a Turbine Rotor Passage, *Part-1 Separate Effects*", ASME paper 92-GT-75.
5. Roback, R.J., Dring, R.P., 1992, "Hot Streaks and Phantom Cooling in a Turbine Rotor Passage, *Part-2 Combined Effects and Analytical Modelling*", ASME paper 92-GT-76.
6. Takanishi, R.K., Ni, R.H., 1990, "Unsteady Euler Analysis of the Redistribution of an Inlet Temperature Distortion in a Turbine, AIAA paper 90-2262.
7. Dorney, D.J., Davis, R.L., Edwards, D.E., Madavan, N.K., 1990, "Unsteady Analysis of Hot Streak Migration in a Turbine Stage", AIAA-90-2354.
8. Dorney, D.J. and Schwab, R.J., 1995, "Unsteady Numerical Simulations of Radial Temperature Profile Redistribution in a Single Stage Turbine", ASME paper 95-GT-178.
9. Yoshino, S., 2002, "Heat Transfer in Rotating Turbine Experiments", D.Phil. Thesis, Oxford University.
10. Thorpe, S.J., Yoshino, S., Ainsworth, R.W., Harvey, N.W., 2005, "The Effect of Work Processes on the Casing heat Transfer of a Transonic Turbine", ASME Journal of Turbomachinery, Vol.128, pp. 1-8.
11. Thorpe, S.J., Yoshino, S., Ainsworth, R.W., Harvey, N.W., 2004, "An Investigation of the Heat Transfer and Static Pressure on the Over-tip Casing Wall of an Axial Turbine Operating at Engine Representative Flow Conditions: *Part II, Time-resolved Results*", International Journal of Heat and Fluid Flow, Vol. 25 (6), pp. 945-960.
12. Rhee, D. and Cho, H.H., 2005, "Local Heat/Mass Transfer Characteristics on a Rotating Blade with Flat Tip in a Low Speed Annular Cascade: Part 2- Tip and Shroud", ASME paper GT2005-68724.

13. Camci, C., 2004, "Experimental and Computational Methodology for Turbine Tip De-sensitization", *VKI Lecture Series 2004-02*, Turbine Blade Tip Design and Tip Clearance Treatment, 2004.
14. Rao, M.N., Gumusel, B., Kavurmacioglu, L., and Camci, C., 2006, "Influence of Casing Roughness on the Aerodynamic Structure of Tip Vortices in an Axial Flow Turbine", ASME paper GT 2006-91011.
15. Kline, S.J., McClintock, F.A., 1953, "Describing Uncertainties in Single-Sample Experiments", Mechanical Engineering, Vol.75, pp. 3- 11.

Appendix-A Uncertainty Analysis

$$h = \frac{q_{conv} k_{Al}}{k_{Al}(T_H - T_f) - L_{Al} q_{conv}}$$

$$\delta h = \left[\left(\frac{\partial h}{\partial q} \delta q \right)^2 + \left(\frac{\partial h}{\partial k} \delta k \right)^2 + \left(\frac{\partial h}{\partial T_H} \delta T_H \right)^2 + \left(\frac{\partial h}{\partial T_f} \delta T_f \right)^2 + \left(\frac{\partial h}{\partial L} \delta L \right)^2 \right]^{1/2}$$

$\delta q = \delta q_{conv}$

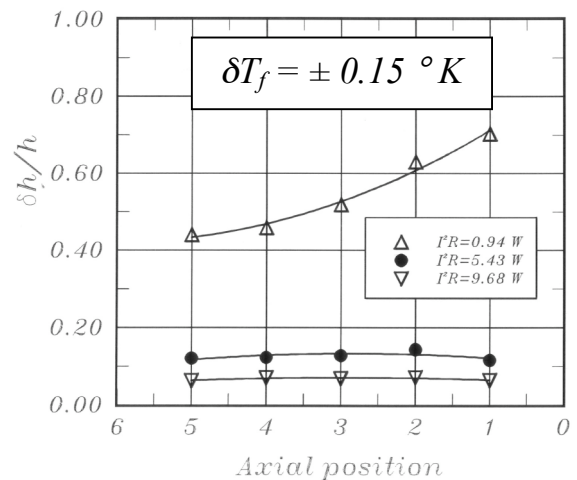
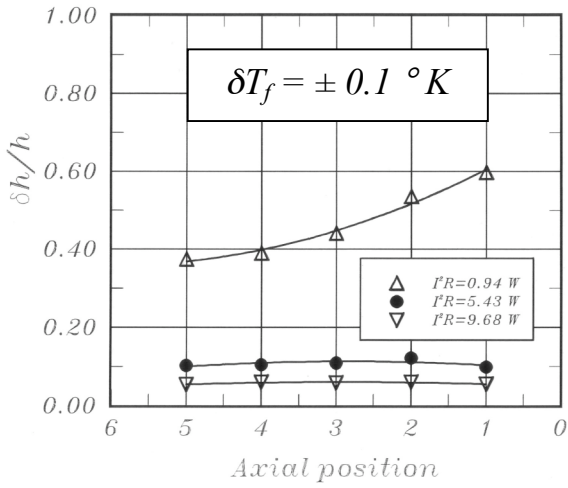


Figure 14 Influence of reference temperature measurement error δT_f on $\delta h/h$
 $\delta q_{conv}/q_{conv} = \pm 0.01$, $\delta k = \pm 0.221 \text{ W/mK}$, $\delta L = \pm 25 \mu\text{m}$ (0.001 mils)

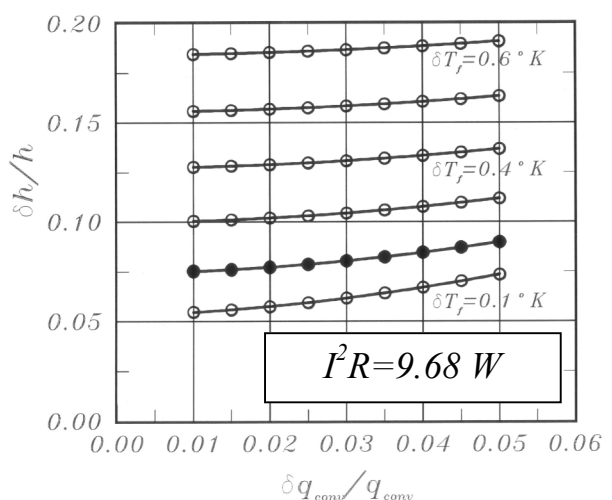
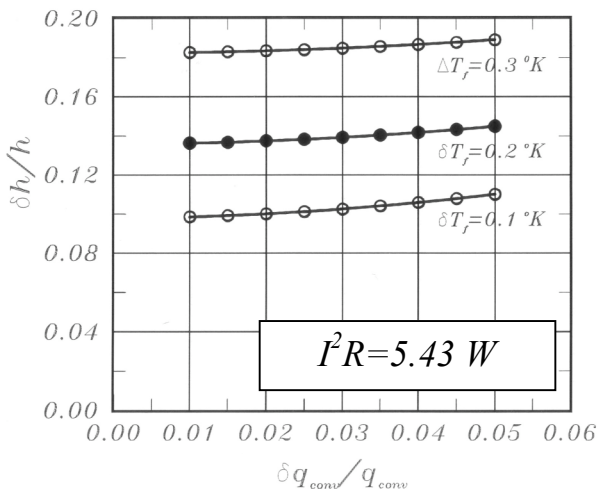


Figure 15 Influence of heater power setting on $\delta h/h$
 $\delta T_H = \pm 0.15 \text{ }^{\circ}\text{K}$, $\delta k = \pm 0.221 \text{ W/mK}$, $\delta L = \pm 25 \mu\text{m}$ (0.001 mils)